INTRINSIC EMITTANCE REDUCTION IN TRANSMISSION MODE PHOTOCATHODES*

Hyeri Lee†, Luca Cultrera, Ivan V. Bazarov, CLASSE, Ithaca, NY 14853, USA

Abstract

High quantum efficiency (QE) and low emittance electron beams provided by multi-alkali photocathodes make them of great interest for next generation high brightness photoinjectors. Spicer's three-step model well describe the photoemission process, however, some photocathode characteristics such as their thickness have not been completely exploited to further improve the brightness of the generated electron beam. In this work, we report on the emittance and QE of a multi-alkali photocathode grown onto glass substrate operated in transmission and reflection modes at different photon energies. We observed a 20% reduction on the intrinsic emittance from the reflection to the transmission mode operation. This observation can be explained by inelastic electron-phonon scattering events experienced by electrons during their transit towards the cathode surface. This scattering will expect the further emittance reduction than the no scattering at the cryo-temperatures.

INTRODUCTION

Alkali antimonides photocathodes [1, 2] have already demonstrated their potential as photoelectron sources for the generation of high brightness beams for next generation light sources like Energy Recovery Linacs [3] and Free Electron Lasers [4]. When operated with photon energy close to their workfunction these photocathodes can provide electron beams suitable for ultrafast electron diffraction (UED) or ultrafast electron microscopy by having a lower intrinsic emittance and higher QE's compared to those of metals [5]. The intrinsic emittance can be expressed as a function of the mean trasnsverse energy (MTE) of emitted electrons at the photocathode surface as $\epsilon_{i,x} = \sigma_x \sqrt{\text{MTE}/m_e c^2}$ where $\epsilon_{i,x}$ is the rms normalized transverse emittance in the x-plane at the photocathode surface, σ_x is the rms laser spot size, $m_e c^2$ is the rest mass energy of the free electron.

Theories of photoemission are based on the Spicer's three-step model [6], where QE and intrinsic emittance of metal photocathodes have been predicted with the Fermi-Dirac (FD) distribution [7, 8]. By taking a finite temperature of the electron gas into consideration [8], experimental data can be better explained near the emission threshold and below the threshold for both metals [9] and semiconductors [1, 10]. However, estimates of energy losses due to electron-phonon (e-ph) interactions are not considered where these interactions are dominant for semiconductors near the emission threshold. In this region, electrons slowly relax through e-ph
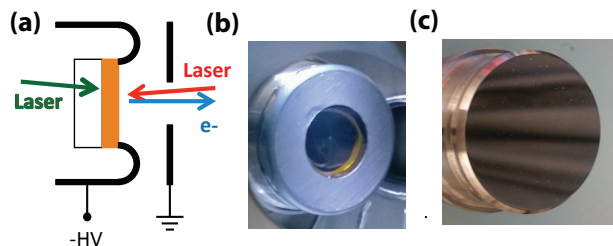
Figure 1: (a) A schematic for direction of light and photoelectrons: green arrow for transmission mode, red arrow for reflection mode. (b) a photocathode used in the experiment with a glass in the middle (c) typical photocathode (only reflection mode is allowed)

scattering losing a small amount of energy during each event. This effect is amplified the longer electrons have to travel in the material before the emission. Travel distances before emission can be increased by operating a photocathode in transmission mode. A schematic for both transmission and reflection mode is shown in Fig. 1(a). Because the emission occurs at the photocathode-vacuum interface, electrons generated in the transmission mode must travel longer distances through the material before their emission resulting in smaller MTEs.

In this paper, we report on the QE and MTE of a $Na_2KSb:Cs_3Sb$ photocathode for reflection and transmission modes, both performed on the same photocathode at different laser wavelengths. Analytical and numerical models of electron transport, which include e-ph scattering to account for the energy loss during electron's travel to the photocathode surface well reproduce the experimental data.

EXPERIMENTS

Growth

The $Na_2KSb:Cs_3Sb$ was grown in a UHV chamber using vapors generated by effusion cells loaded with pure metals [11]. In order to operate the photocathode also in transmission mode a 2.5 mm thick Borofloat 33 glass was used as a substrate. The metallic substrate holder is hollow allowing the transmission mode operation by passing light through the back of the substrate as shown in Fig. 1(b).

Emittance and QE measurement

A high voltage DC gun operated at 150, 200 and 250 kV was used in the emittance measurement (with corresponding electric fields at the cathode surface ranging between 1.7 and 2.8 MV/m. A detailed description of the DC gun and the experimental beamline can be found elsewhere [12].The

solenoid scan technique was used to determine the emittance of the electron beam while operating the photogun with small laser diode modules. Detailed description of the method and measurement error propagation can be found elsewhere [10]. Three laser apertures and three different gun voltages were used to verify the linear relationship between rms emittance value and rms spot size and to obtain intrinsic emittance as a function of the electric field. Electron beam measurements have been performed using three different wavelengths chosen based on available diode lasers: 780, 690 and 532 nm.

The QE of the photocathode is obtained by measuring the photocurrent collected by a Faraday cup downstream of the gun using a picoammeter and by estimating the laser power incident on the photocathode surface using the laser power measured just before the last UHV window taking also into account all the transmission coefficient of the glass and the reflectivity of the UHV mirrors as a function of the different wavelengths. For the transmission mode cathode the transmission of the Borofloat 33 glass substrate (>95% in the 500-800 nm spectral range) has been included.

RESULTS AND SIMULATION

Photoelectrons' MTEs derived from the emittance measurements along with the QEs of the $Na_2KSb:Cs_3Sb$ in transmission and reflection mode are reported in Table 1 and Fig. 2 respectively. MTEs for all data were consistant within errors among all electric fields. A consistent MTE decrease (about 20%, see Table 1) is also observed when the cathode is operated in the transmission rather than the reflection mode for all the laser wavelengths used in the experiment.

Wavelength (nm)	Reflection (meV)	Transmission (meV)	Reduction (meV)
532	200±4	166±3	34±7
690	62±3	53±3	9±6
780	40±2	33±2	7±4

Table 1: Measured MTE for reflection and transmission modes at different laser wavelengths.

In order to estimate the expected values of MTEs, first we have derived analytical formulas using the Spicer's three-step model that also takes into account inelastic phonon scattering experienced by the electrons. The photon absorption is calculated from the complex index of refraction [13] assuming negligible absorption in the Cs_3Sb layer. The initial electron distribution is represented by an exponential decay function vs. the distance from the photocathode light-exposed surface. Electrons then have to drift towards the appropriate cathode interface in order to be extracted. These expressions do not take the finite temperature of the electron gas into account, but are useful to estimate photoelectrons' intrinsic emittance when excited far from the threshold [14].
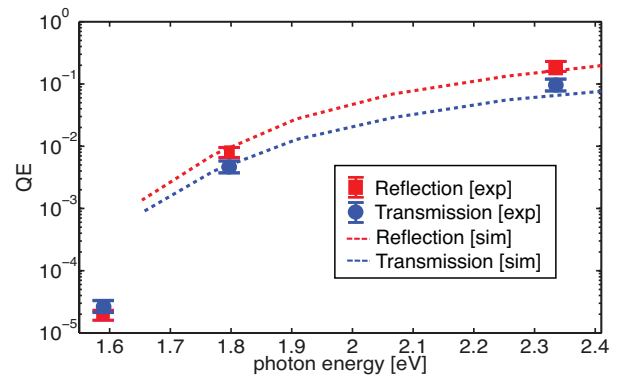

Figure 2: Quantum efficiency as a function of photon energy. The QE data (dot) at each wavelength are measured at 250 kV. The simulation QE is presented in the dotted line (the QE was scaled with a scaling coefficient.)

Parameter	Value
l_{mfp} [15]	25nm
$\overline{dE}$ [16]	22meV
thickness	150nm
E_w	1.6eV

Table 2: Parameters used in the simulation. l_{mfp} is the mean free path of e-ph collisions, $\overline{dE}$ is the average energy loss per collision, E_w is work function.

A Monte-Carlo simulation was performed in order to better reproduce the measured MTEs near the emission threshold. Electrons were randomly generated as a function of the photon wavelength following a FD distribution. Inset in Fig. 3 shows an example of this distribution in energy. Electrons experience scattering events losing $\overline{dE}$ for each collision. Path lengths x between successive collisions are randomly sampled based on a form of $e^{-x/l_{mfp}}$ [17]. Once an electron reaches the vacuum interface it is emitted if its longitudinal energy is larger than E_w where the parameters are in Table 2. MTE of the extracted electrons is then computed. The transverse energy is assumed to be conserved during the emission process. The results are shown in Fig. 3. An excellent agreement can be seen between the Monte-Carlo simulations that now include both e-ph scattering and the effect of finite temperature of the electron gas.

The MTE reduction observed in these measurements can thus be explained by the increased number of inelastic e-ph scattering events when operating the photocathode in the transmission mode. The simulations also well explain why the absolute measured MTE lowers at longer laser wavelengths as the absorption coefficient gets smaller there. QE lowering up to 50% are measured in agreement with simulation when a 150 nm thick cathode is operated in transmission rather than reflection mode as shown in Fig. 2. Larger losses, up to 2 orders of magnitude, are expected from 500 nm thick cathodes.
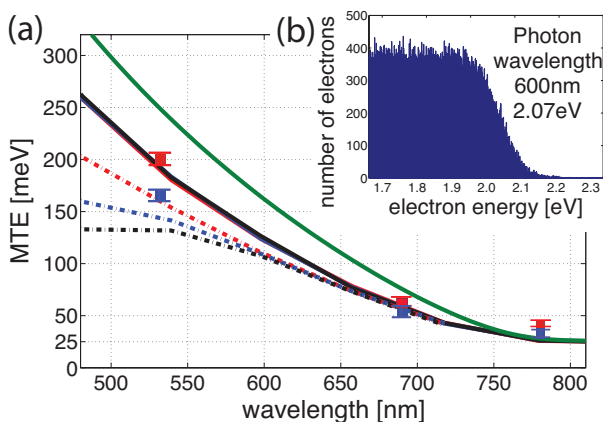
Figure 3: (a) MTE from Monte-Carlo simulations and experimental data (reflection (red dot) and transmission (blue dot)) as a function of laser wavelength at three different photocathode thicknesses: 150(red), 300(blue) and 500(black) nm. Dotted lines represent the transmission mode. The green line is calculated with the model from Ref. [8]. (b) A histogram of excited electrons above E_w following a FD distribution at room temperature.
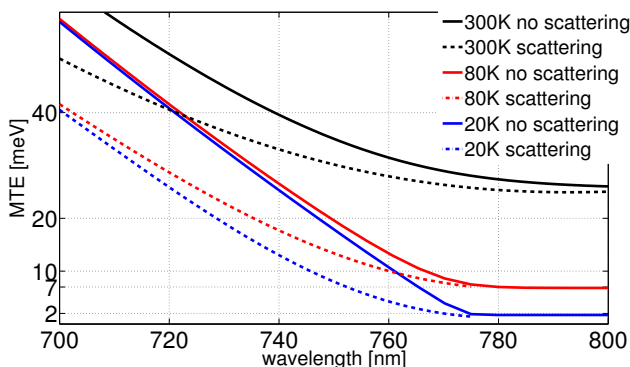

Figure 4: MTE at different temperatures (300K, 80K and 20K). The solid lines represent MTEs from no scattering [8]; The dotted lines show MTEs from simulation using scattering with 150nm thickness, reflection cathode.

FUTURE PLANS AND CONCLUSION

In the near term, experiments will continue towards cooling down the transmission photocathodes. Transverse Energy Meter (TEmeter) connected to a growth chamber under UHV supports cooling of the photocathodes from room temperature (300K) to cryogenic temperature (90K). This device has also demonstrated to measure a ultra low emittance(< 0.4mm-mrad per mm) or equivalently, low MTE (below 100meV) as low as 22 ± 1meV from a cryo-cooled photocathode. [1, 10] With this device, it will show changes of the emittance and QE at 90K near the emission threshold for the transmission cathode.

The main upgrade plan is to build a new DC gun with a cryogenic cooling capacity down to 20K that can operate near 200kV. At 200kV, this will result in a reasonable field level of 10MV/m. It will not only minimize the emittance growth due to space charge effect for UED operation, but also maximize the charges extracted from the photocathodes. As shown in Fig. 4 the MTE can be as small as 2meV at 20K near the emission threshold and the simulation predicts the lower MTE with the inelastic e-ph scattering. Also coherence lengths in the order of 10s of nm can be possible with initial beam size of $100\mu m$, MTE of 5meV and 100 fs final bunch length [18]. The successful generation of electron bunches compatible with UED for imaging of molecular and atomic motion requires sources capable of providing photoelectrons with extremely low MTE and a small initial laser beam size (tens of microns). This DC gun will provide great opportunities to study the photoemission process even at the cryogenic temperature and to generate electron beams suitable for UED experiments [18].

We aim to improve our understanding of the photoemission process to generate and to measure electrons with the lowest possible emittance with reasonable QE. Work is in progress to achieve the emittance as low as possible by using a transmission mode photocathode, cooling down the photocathode and increasing the voltage and electric field of the photoinjector.

REFERENCES

[1] L. Cultrera *et al.*, Phys.Rev.ST Accel.Beams 18,113401 (2015)

[2] S. Schubert *et al.*, APL Mater.1,032119 (2013)

[3] B. Dunham *et al.*, Appl.Phys.Lett. 102,034105 (2013)

[4] C. Gulliford *et al.*, Appl.Phys.Lett. 106,094101 (2015)

[5] J. Maxson *et al.*, Appl.Phys.Lett. 106,234102 (2015)

[6] W. E.Spicer, Phys. Rev. 112,114 (1958)

[7] D. H. Dowell and J. F. Schmerge, Phys.Rev.ST Accel.Beams 12,074201 (2009)

[8] T. Vecchione and D. Dowell, Proceedings of FEL2013, New York, NY, USA, FEL Technology I: Guns, Injectors and Accelerator (2013), pp. 424–426

[9] J. Feng *et al.*, Rev.Sci.Instrum.86,015103 (2015)

[10] H. Lee *et al.* Rev.Sci.Instrum.86.073309 (2015)

[11] L. Cultrera *et al.* J.Vac.Sci.Technol.,B 34,011202 (2016)

[12] J. Maxson *et al.*, Rev.Sci.Instrum.85,093306 (2014)

[13] A. Ebina *et al.*, Phys.Rev.B 7,4712 (1973)

[14] H. Lee *et al.*, Appl.Phys.Lett. 108, 124105 (2016)

[15] K. L. Jensen *et al.*, J.Appl.Phys. 104, 044907 (2008)

[16] M. B. Tzolov *et al.*, Thin Solid Films 213,99 (1992)

[17] R. Feynman *et al.*, The Feynman Lectures on Physics, 2nd ed. Addision-Wesley, Boston, 1963. Vol.1.

[18] C. Gulliford, e-printhttp://arxiv.org/abs/1510. 07738